

^{123}I -ITdU–Mediated Nanoirradiation of DNA Efficiently Induces Cell Kill in HL60 Leukemia Cells and in Doxorubicin-, β -, or γ -Radiation–Resistant Cell Lines

Sven N. Reske, Sandra Deisenhofer, Gerhard Glatting, Boris D. Zlatopolskiy, Agnieszka Morgenroth, Andreas T. J. Vogg, Andreas K. Buck, and Claudia Friesen

Nuclear Medicine Clinic, Universität Ulm, Ulm, Germany

Resistance to radiotherapy or chemotherapy is a common cause of treatment failure in high-risk leukemias. We evaluated whether selective nanoirradiation of DNA with Auger electrons emitted by 5- ^{123}I -iodo-4'-thio-2'-deoxyuridine (^{123}I -ITdU) can induce cell kill and break resistance to doxorubicin, β -, and γ -irradiation in leukemia cells. **Methods:** 4'-thio-2'-deoxyuridine was radiolabeled with $^{123}\text{I}/^{131}\text{I}$ and purified by high-performance liquid chromatography. Cellular uptake, metabolic stability, DNA incorporation of ^{123}I -ITdU, and the effect of the thymidylate synthase (TS) inhibitor 5-fluoro-2'-deoxyuridine (FdUrd) were determined in HL60 leukemia cells. DNA damage was assessed with the comet assay and quantified by the olive tail moment. Apoptosis induction and irradiation-induced apoptosis inhibition by benzoylcarbonyl-Val-Ala-Asp-fluoromethyl ketone (z-VAD.fmk) were analyzed in leukemia cells using flow cytometry analysis. **Results:** The radiochemical purity of ITdU was 95%. Specific activities were 900 GBq/ μmol for ^{123}I -ITdU and 200 GBq/ μmol for ^{131}I -ITdU. An in vitro cell metabolism study of ^{123}I -ITdU with wild-type HL60 cells demonstrated an uptake of 1.5% of the initial activity/ 10^6 cells of ^{123}I -ITdU. Ninety percent of absorbed activity from ^{123}I -ITdU in HL60 cells was specifically incorporated into DNA. ^{123}I -ITdU caused extensive DNA damage (olive tail moment > 12) and induced more than 90% apoptosis in wild-type HL60 cells. The broad-spectrum inhibitor of caspases zVAD.fmk reduced ^{123}I -ITdU-induced apoptosis from more than 90% to less than 10%, demonstrating that caspases were central for ^{123}I -ITdU-induced cell death. Inhibition of TS with FdUrd increased DNA uptake of ^{123}I -ITdU 18-fold and the efficiency of cell kill about 20-fold. In addition, ^{123}I -ITdU induced comparable apoptotic cell death (>90%) in sensitive parental leukemia cells and in leukemia cells resistant to β -irradiation, γ -irradiation, or doxorubicin at activities of 1.2, 4.1, 12.4, and 41.3 MBq/mL after 72 h. This finding indicates that ^{123}I -ITdU breaks resistance to β -irradiation, γ -irradiation, and doxorubicin in leukemia cells. **Conclusion:** ^{123}I -ITdU-mediated nanoirradiation of DNA efficiently induced apoptosis in sensitive and resistant leukemia cells against doxorubicin, β -irradiation, and γ -irradiation and may provide a novel treatment strategy for

overcoming resistance to conventional radiotherapy or chemotherapy in leukemia. Cellular uptake and cell kill are highly amplified by inhibiting TS with FdUrd.

Key Words: Auger radiation; nuclear targeting; treatment; DNA nanoirradiation; chemoresistance; radioresistance

J Nucl Med 2007; 48:1000–1007

DOI: 10.2967/jnumed.107.040337

Chemoresistance and radioresistance are major obstacles to successful induction of long-term survival in high-risk leukemia. Inhibition of tumoral DNA synthesis with antimetabolites targeting specific key enzymes of thymidine metabolism or DNA synthesis is an effective, safe, and well-established strategy for antineoplastic chemotherapy. However, most neoplasms ultimately develop resistance to radiotherapy or chemotherapy, resulting in progressive, uncontrolled proliferation of neoplastic cells and finally patient death. Therefore, cytotoxic drugs with the potential to kill resistant cancer cells are needed.

In this study, we report extremely high cytotoxicity for selective ultra-short-ranged Auger electron–mediated nanoirradiation delivered by 5- ^{123}I -iodo-4'-thio-2'-deoxyuridine (^{123}I -ITdU), metabolically incorporated into DNA. Auger electrons are known to generate clusters of high ionization density, inducing base damage, single-strand breaks, double-strand breaks, and multiple damaged sites (1–3). The low energy of Auger electrons, ranging from a few electron volts up to 100 keV (4), and their short pathlength of only several nanometers in water, limit dense ionizations and extensive DNA damage within a sphere of a few nanometers around the emission center (5), whereas cytosolic or extracellular decays of Auger emitters are 10–100 times less radiotoxic (6).

The radiolabeled thymidine analog ^{123}I -ITdU (Fig. 1) was used as a molecular carrier for the Auger electron–emitting radiohalogen ^{123}I into DNA. ^{123}I -ITdU was selected because

Received Feb. 1, 2007; revision accepted Mar. 16, 2007.

For correspondence or reprints contact: Sven N. Reske, MD, Universität Ulm, Klinik für Nuklearmedizin, Robert-Koch-Strasse 8, D-89081 Ulm, Germany.

E-mail: sven.reske@uniklinik-ulm.de

COPYRIGHT © 2007 by the Society of Nuclear Medicine, Inc.

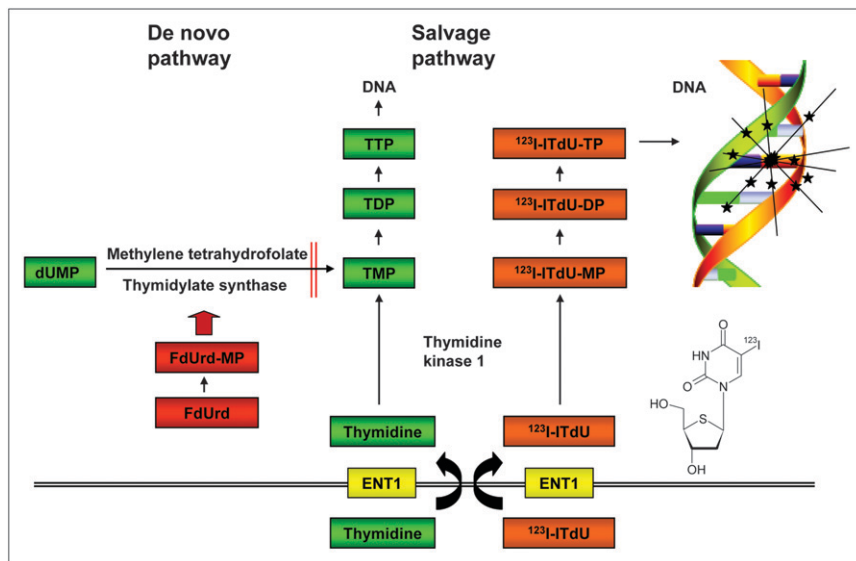


FIGURE 1. Thymidine de novo and salvage pathways. Thymidine de novo pathway is blocked by FdUrd, considerably enhancing flux of thymidine and ^{123}I -ITdU through salvage pathway and, thus, ^{123}I -ITdU incorporation into DNA.

it is specifically incorporated into nuclear DNA through the thymidine salvage pathway (7–9), has no selectivity for mitochondrial DNA, and is metabolically more stable than other 5-halogeno-substituted deoxyuridines (3,8–10).

In this study, we showed highly efficient DNA damage and apoptosis induction triggered by ^{123}I -ITdU incorporated into DNA both in sensitive and in β - or γ -irradiation and doxorubicin-resistant leukemia cell lines. As has been shown for IuDR (11,12), metabolic stabilization of ITdU by inhibiting thymidylate synthase (TS) activity with 5-fluoro-2'-deoxyuridine (FdUrd) highly increased cellular uptake, DNA incorporation, and ^{123}I -ITdU-induced apoptosis.

MATERIALS AND METHODS

Chemicals

Chemicals and solvents were purchased from Sigma-Aldrich and Merck, or otherwise as indicated. All reagents and solvents were of the highest commercially available grade and used without further purification. No-carrier-added sodium ^{131}I -iodide was obtained from Amersham Biosciences, and no-carrier-added sodium ^{123}I -iodide was purchased from Zyklotron AG. The 5-trimethylstannyl precursor of ITdU and the standard compound ITdU were synthesized according to previously reported methods (8,13–15).

Synthesis of ^{123}I -ITdU and ^{131}I -ITdU

Fifteen microliters of chloramine-T (0.5 mg/mL in 66% methanolic solution) were added to a reaction vial containing 35 μL of no-carrier-added $^{123/131}\text{I}$ -NaI (1,200 MBq in 0.05 M NaOH) and 0.14 mg of precursor in 60 μL of buffer (1 M H_3PO_4 , pH 2, in 40% methanolic solution). The reaction was stopped after 15 min by adding 25 μL of 0.1 thiosulfate solution in 50% methanolic solution. The radiochemical yield was 95%. $^{123/131}\text{I}$ -ITdU was purified via semipreparative high-performance liquid chromatography (HPLC) (sample loop, 200 μL ; eluent, MeOH/ H_2O 30/70 v/v; flow, 2 mL/min; column, LiChrospher 100 RP-18 [Agilent Technologies], 5 μm , 250 \times 8 mm). For isolation of the product, the fraction between 10 and 13 min was collected, and 100 μL of a 10 mM methionine solution were added. The product volume of

about 5 mL was reduced by evaporation at 80°C at reduced pressure (nitrogen flow and vacuum). The product was redissolved in 100 μL of water for injection and incubated for 15 min with anion exchange beads (Amberlite IRA-958, 13-45 mesh, acrylic resin, strong basic, Cl^- form). The supernatant was removed, the resin washed with another 100 μL , and the combined solutions passed through a sterile filter. The overall radiochemical yield was 20%. For production of high-activity doses of ^{123}I -ITdU, 37 μL of chloramine-T solution were added to a mixture of 140 μL of buffer, 4.7 μL of precursor solution (48 mg of buffer per milliliter) and 82 μL of ^{123}I -NaI (5 GBq in 0.05 M NaOH). At a reaction time of 15 min, the total volume was injected onto a C4 reversed-phase column (sample loop, 500 μL ; eluent, EtOH/ H_2O 10/90 v/v; flow, 1 mL/min; column, Kromasil 100-5 μ , C4 [Eka Chemicals], 250 \times 4 mm). The peak fraction was made isotonic using a 10% NaCl solution and further diluted with isotonic saline to the desired activity concentration. For this procedure, overall radiochemical yield was 80%. Quality control for each procedure was conducted using HPLC (eluent, MeOH/ H_2O 20/80 v/v; flow, 1 mL/min; column, LiChrospher 100 RP-18, 5 μm , 250 \times 4 mm).

Cell Lines

The human myeloid leukemic cell line HL60 and the human lymphoblastic leukemia T cells CEM were grown in RPMI 1640 (Gibco BRL) containing 10% fetal calf serum (Biochrom); 10 mM *N*-(2-hydroxyethyl)piperazine-*N'*-(2-ethanesulfonic acid), pH 7.3 (Biochrom); 100 U of penicillin per milliliter (Gibco); 100 μg of streptomycin per milliliter (Gibco); and 2 mM L-glutamine (Biochrom). HL60^{gammaR}, a variant of HL60 that is resistant to a radiation-absorbed dose of up to 10 Gy (^{60}Co , 0.4 Gy/min) (16), and HL60^{betaR}, a variant of HL60 that is resistant to a radiation-absorbed dose of up to 10 Gy applied by β -irradiation (^{90}Y , 87.6 MBq/100 mL, incubation for 24 h), were generated for more than 12 mo (16). To preserve the resistance of these cell lines, HL60^{gammaR} was irradiated with γ -irradiation (^{60}Co) and HL60^{betaR} was irradiated with β -irradiation (^{90}Y) every 4 wk by applying a radiation-absorbed dose of 10 Gy. CEM^{doxoR}, a variant of CEM resistant toward doxorubicin, was generated by continuous culture in doxorubicin (0.1 $\mu\text{g}/\text{mL}$) for more than 12 mo. For the experiments,

CEM^{DoxoR} cells were washed and cultured for 2 wk in the absence of doxorubicin (17). All cell lines were mycoplasma-free.

Cellular Uptake and DNA Incorporation of ¹²³I-ITdU

HL60 cells (1×10^6 /mL) were preincubated in the absence or presence of FdUrd (0.01 nmol/L) for 1 h before incubation with 0.5 MBq of ¹²³I-ITdU, and the cells were incubated at 37°C with 5% CO₂ for 2 h and 24 h. After incubation, the medium was removed and the cells were washed 3 times with ice-cold phosphate-buffered saline (PBS). After washing, the cells were harvested and collected by centrifugation. The radioactivity of the cell pellet was measured in a γ -scintillation counter (Auto- γ -5003; Canberra Packard).

DNA Uptake

Cultured HL60 cells were harvested and seeded at a concentration of 1×10^6 into 24-well plates. HL60 cells (1×10^6 /mL) were preincubated in the absence or presence of FdUrd (0.01 nmol/L) for 1 h before incubation with 0.5 MBq of ¹²³I-ITdU, and the cells were incubated at 37°C with 5% CO₂ for 2 h and 24 h. After incubation, the medium was removed and the cells were washed 3 times with ice-cold PBS. After washing, the cells were centrifuged for 5 min at 300g, and the cell pellets were resuspended in 200 μ L of PBS. DNA was extracted using the DNeasy Tissue Kit from Qiagen. In brief, cell pellets resuspended in 200 μ L of PBS were incubated with 4 μ L of RNase (100 mg/mL; Qiagen) for 2 min at room temperature to get RNA-free genomic DNA. Then, 20 μ L of proteinase K and 200 μ L of buffer AL from the DNeasy Tissue Kit were added to the sample, mixed thoroughly in a vortex mixer, and incubated at 70°C for 10 min. After incubation, 200 μ L of 96% ethanol were added to the sample and mixed thoroughly in a vortex mixer. Then, the mixture was pipetted into the DNeasy Mini spin column, placed in a 2-mL collection tube, and centrifuged at 6,000g for 1 min. After centrifugation, the flow-through and collection tubes were discarded. The DNeasy Mini spin column was placed in a new collection tube, 500 μ L of buffer AW1 (DNeasy Tissue Kit) were added, and the column was centrifuged for 1 min at 6,000g. After centrifugation, the flow-through and collection tubes were discarded. The DNeasy Mini spin column was placed in a new collection tube, and 500 μ L of buffer AW2 (DNeasy Tissue Kit) were added and centrifuged for 3 min at 20,000g to dry the DNeasy membrane. After centrifugation, the flow-through and collection tubes were discarded. The DNeasy Mini spin column was placed in a clean 1.5-mL microcentrifuge tube, and 200 μ L of buffer AE (DNeasy Tissue Kit) were pipetted directly onto the DNeasy membrane, followed by incubation for 1 min at room temperature and then centrifugation for 1 min at 6,000g to elute the DNA. Radioactivity in the DNA was measured in a γ -scintillation counter (Auto- γ -5003).

Metabolic Stability of ¹²³I-ITdU

For in vitro stability of ¹²³I-ITdU, 10^6 HL60 cells were incubated with a 0.5 MBq/mL concentration of ¹²³I-ITdU in the absence or presence of FdUrd (0.01 nmol/L). The extent of ¹²³I-ITdU deiodination was determined by reversed-phase HPLC analysis of cell supernatant aliquots after 2 h and 21 h of incubation. Analytic HPLC system 1100 from Agilent was used with a quaternary low-pressure gradient pump, a 1-channel UV-VIS detector using 290 nm, and a final NaI detector-type GABI from Raytest for detection of γ -radiation. The radiochemical yields of all reaction products were obtained as the relative peak area fraction of the sum of all areas in the radiochromatogram. Complete elution was checked by analyzing the same sample amount choosing a column bypass.

Measurement of DNA Damage (Comet Assay)

DNA damage (DNA breaks) was measured by the alkaline comet assay as previously described (18). In brief, 10 μ L of cell suspension (10,000 cells) from treated and untreated cells were resuspended in 120 μ L of low-melting agarose at 37°C. One hundred microliters of this suspension were spotted onto a microscope slide and covered with a cover slide. After the slide had been kept on ice for 5 min in the dark, the cover slide was removed and the slide was incubated overnight in lysis buffer containing 2.5 M NaCl, 100 mM ethylenediaminetetraacetic acid, 10 mM Tris, and 1% Na-laurylsarcosinate, pH 10. Thereafter slides were preincubated in electrophoresis buffer (300 mM NaOH and 1 mM ethylenediaminetetraacetic acid, pH > 13) for 25 min, and electrophoresis was performed for 25 min (25 V, 300 mA). The slides were neutralized in 0.4 M Tris, pH 7.5, washed in distilled water, fixed in 100% ETOH for 5 min, and air-dried overnight. Analysis after staining with ethidium bromide (20 μ g/mL) was performed on a fluorescence microscope using a charge-coupled-device camera connected to a personal computer and analysis software. Relative DNA breakage was expressed as the olive tail moment, which was determined by measuring the fluorescence intensity of the tail and nucleus using Kinetic Imaging Komet 5.0 software (BFI Optilas).

Apoptosis Induction of ¹²³I-ITdU

Leukemia cells (2×10^5 cells in 1 mL) were incubated with a 0.0041, 0.012, 0.041, 0.12, 0.41, 1.2, 4.1, 12.4, or 41.3 MBq/mL concentration of ¹²³I-ITdU, ¹³¹I-ITdU, or sodium ¹²³I-iodide or were treated with a 0.01, 0.1, 1, 10, or 100 μ g/mL concentration of nonradioactive ¹²⁷I-ITdU as a control in a 150-mL flask or 96-well plates for 72 h. Activities of ¹³¹I and ¹²³I were applied in a 1-mL volume. After irradiation, apoptosis was quantified by flow cytometry as previously described (19). In brief, to determine apoptosis, the cells were lysed with Nicoletti buffer containing 0.1% sodium citrate plus 0.1% Triton X-100 (Union Carbide Corp.) and propidium iodide (50 μ g/mL), as described by Nicoletti et al. (19). The percentage of apoptotic cells was measured by hypodiploid DNA (subG1) or forward scatter/side scatter analysis. Propidium iodide-stained nuclei or the forward scatter/side scatter profile of cells was analyzed by flow cytometry (FACSCalibur; Becton Dickinson).

Inhibition of Irradiation-Induced Apoptosis by z-VAD.fmk

Caspase activation was inhibited as previously described (20). In brief, the broad-spectrum tripeptide inhibitor of caspases benzoylcarbonyl-Val-Ala-Asp-fluoromethyl ketone (z-VAD.fmk; Enzyme Systems Products) was used at a concentration of 50 μ mol/L. HL60 cells were preincubated with z-VAD.fmk 1 h before ¹²³I-ITdU incubation. After 72 h, the percentage of apoptotic cells was measured by hypodiploid DNA (subG1) or forward scatter/side scatter analysis. Propidium iodide-stained nuclei or the forward scatter/side scatter profile of cells was analyzed by flow cytometry (FACSCalibur).

Dose-Effect Analysis

For densely ionizing radiation (Auger electron emitters), an exponential model appropriately describes the relationship between radioactivity concentration C (MBq/mL) and the number of surviving cells N (5); that is, $N = N_0 \cdot \exp(-\alpha \cdot C)$, with N_0 being the number of cells surviving the procedure as described above and α describing the sensitivity against the applied radiolabeled compound or treatment.

Statistical Analysis

The percentage of specific cell death was calculated as $100 \times (\text{experimental dead cells [\%]} - \text{spontaneous dead cells in medium [\%]} / (100\% - \text{spontaneous dead cells in medium [\%]})$. Data are given as the mean of triplicates. Similar results were obtained in 3 independent experiments.

Nonlinear curve fitting for the dose-effect analysis was performed using GraphPad Prism (GraphPad Software), version 4.03, for Windows (Microsoft). To compare different experiments, the ratio of the sensitivity parameter α was calculated applying error propagation.

RESULTS

Radiosynthesis of No-Carrier-Added $^{123}\text{I}/^{131}\text{I}$ -ITdU

Total radiochemical yields were 20% or 80%, depending on the desired final total product volume. Radiochemical purities were more than 95%. Specific activities were 900 GBq/ μmol for ^{123}I -ITdU and 200 GBq/ μmol for ^{131}I -ITdU.

Cellular/DNA Uptake and Cellular Metabolism of ^{123}I -ITdU

Cellular uptake of ^{123}I -ITdU/ 10^6 cells into HL60 cells was about 1.5% of the incubation activity in the medium (Fig. 2A). After 24 h, 90% of internalized activities from ^{123}I -ITdU in HL60 cells were specifically incorporated into DNA (Fig. 2A). However, after the uptake of ^{123}I -ITdU into HL60 cells, ^{123}I -ITdU was mostly deiodinated within 24 h (Fig. 2B). Deiodination of ^{123}I -ITdU was not detectable after incubation of ^{123}I -ITdU in culture medium in the absence of HL60 cells after 24 h.

Enhanced Cellular/DNA Uptake After FdUrd Before Incubation

Inhibition of TS with FdUrd increased cellular uptake of ^{123}I -ITdU. After preincubation with a nontoxic concentration of FdUrd (0.01 nmol/L), incorporation of ^{123}I -ITdU into DNA strongly increased from 1.4% of the dose/ 10^6 cells/24 h in the absence of FdUrd to 25% of the dose/ 10^6

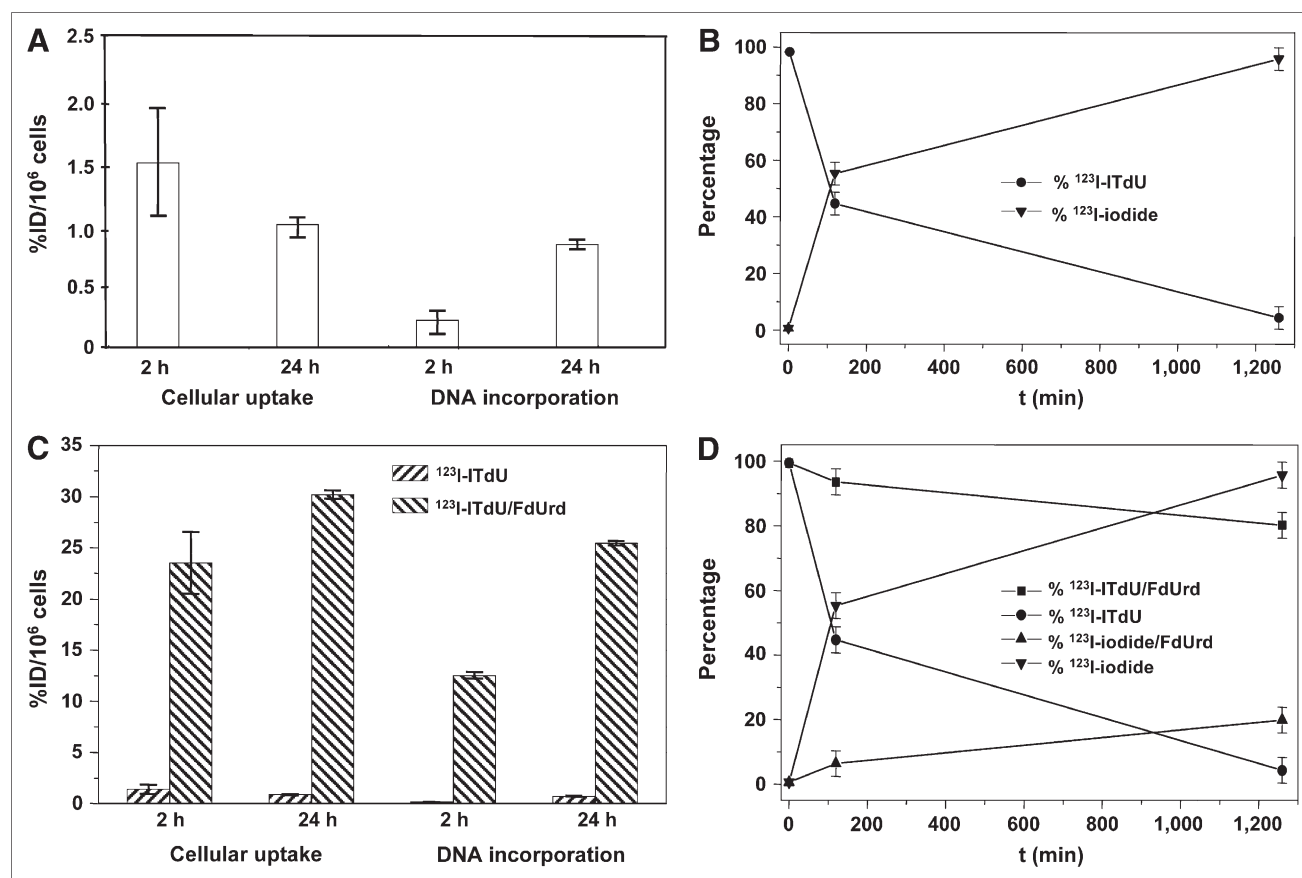


FIGURE 2. (A) Cellular uptake and DNA incorporation of ^{123}I -ITdU. HL60 cells were incubated with 0.5 MBq of ^{123}I -ITdU per milliliter at time points as indicated. (B) In vitro stability of ^{123}I -ITdU. HL60 cells were incubated with 0.5 MBq of ^{123}I -ITdU per milliliter. Extent of ^{123}I -ITdU deiodination was determined by reversed-phase HPLC analysis of cell supernatant aliquots at time points as indicated. (C) Cellular uptake and DNA incorporation of ^{123}I -ITdU with and without TS inhibitor FdUrd. HL60 cells were incubated with 0.5 MBq of ^{123}I -ITdU per milliliter in absence (^{123}I -ITdU) or presence (^{123}I -ITdU/FdUrd) of 0.01 nmol of FdUrd per liter at time points as indicated. (D) In vitro stability of ^{123}I -ITdU. HL60 cells were incubated with 0.5 MBq of ^{123}I -ITdU per milliliter in absence or presence of 0.01 nmol of FdUrd per liter. Extent of ^{123}I -ITdU deiodination was determined by reversed-phase HPLC analysis of cell supernatant aliquots at time points as indicated.

cells/24 h in the presence of FdUrd (Fig. 2C). In addition, inhibition of TS with FdUrd reduced deiodination of ^{123}I -ITdU from 95% to 20% after 24 h (Fig. 2D).

^{123}I -ITdU-Induced DNA Damage

After the application of a 12.4 or 41.3 MBq/mL concentration of ^{123}I -ITdU, metabolically incorporated into the DNA of HL60 cells, a strong induction of DNA damage was found as measured by the Comet assay (Fig. 3A) and quantified by the fluorescence intensity of the tail and nucleus (Fig. 3B) after 0.25, 0.5, 0.75, 1, 2, 3, 4, 5, 6, and 7 h.

^{123}I -ITdU-Induced Apoptosis

HL60 cells were incubated with a 0.0041, 0.012, 0.041, 0.12, 0.41, 1.2, 4.1, 12.4, or 41.3 MBq/mL concentration of ^{123}I -ITdU for 72 h. Roughly 50% apoptotic cell death was measured after incubation of 10^6 HL60 cells with 0.124 MBq/mL (Fig. 4A). In contrast, comparable activities of ^{131}I -ITdU or sodium ^{123}I -iodide could not induce apoptosis. Apoptosis increased to more than 90% when applying 1.2 MBq/mL/ 10^6 cells of ^{123}I -ITdU, whereas apoptosis remained small for ^{131}I -ITdU and sodium ^{123}I -iodide (Fig. 4A). Based on the radioactivity concentration given to the incubation medium, the sensitivity parameter α —a measure of radiosensitivity (5)—for HL60 cells incubated with ^{123}I -ITdU was 50 ± 6 times larger than that for cells incubated with ^{131}I -ITdU (Fig. 4A), emitting mainly β -particles (89%) and conversion electrons (6%) and only 5% Auger electrons (21). The efficiency of cell death induction by ^{123}I -ITdU was 152 ± 18 times higher than that by ^{123}I -iodide not incorporated into DNA (Fig. 4A). Nonradioactive ^{127}I -ITdU, given in a 4- to 5-log higher concentration

to the incubation medium of HL60 cells, compared with ^{123}I -ITdU, induced a maximum of 50% apoptosis up to a concentration of 100 $\mu\text{g}/\text{mL}$ (Fig. 4B). The broad-spectrum inhibitor of caspases zVAD-fmk (50 μM) efficiently inhibited ^{123}I -ITdU-induced apoptosis after irradiation of HL60 cells with a 0.041, 0.012, 0.041, 0.012, 0.41, 1.2, 4.1, 12.4, or 41.3 MBq/mL concentration of ^{123}I -ITdU for 72 h (Fig. 4C).

Amplification of Apoptosis by FdUrd-Mediated Inhibition of TS

Apoptosis induction increased from 4% in cells treated with 0.5 MBq of ^{123}I -ITdU without FdUrd to about 72% in cells additionally treated with FdUrd (0.01 nmol/L) after 24 h (Fig. 5).

Overcoming β -Irradiation, γ -Radiation, and Doxorubicin Resistance with ^{123}I -ITdU

^{123}I -ITdU caused a strong dose- and time-dependent induction of apoptotic cell death—nearly 100%—in HL60^{betaR}, HL60^{gammaR} (Fig. 6A), or CEM^{DoxoR} (20,22) (Fig. 6B) at activities of 0.0041, 0.012, 0.041, 0.12, 0.41, 1.2, 4.1, 12.4, and 41.3 MBq/mL after 72 h. Interestingly, the radiation sensitivity parameter α of HL60^{betaR} cells was a factor of 4.1 ± 0.9 larger than that of HL60^{gammaR} cells toward Auger electron emitter-mediated nanoirradiation delivered by ^{123}I -ITdU (Fig. 6A).

DISCUSSION

^{123}I -ITdU-mediated selective ultra-short-ranged nanoirradiation of DNA was strikingly radiotoxic, leading to early and extensive DNA damage and activated caspases, leading

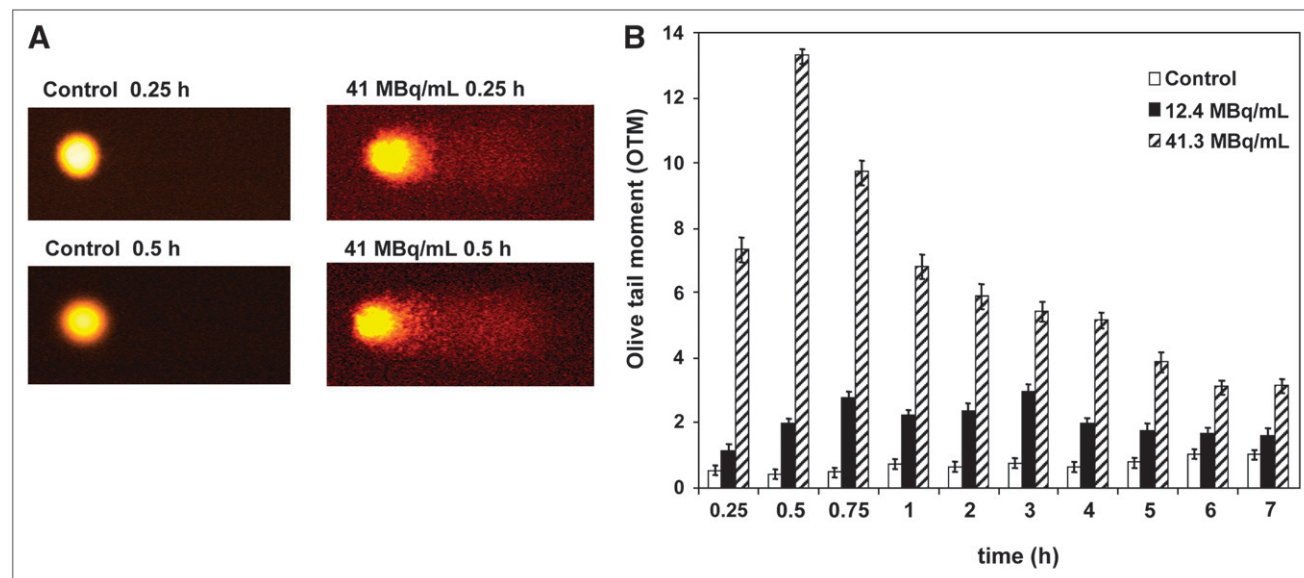


FIGURE 3. ^{123}I -ITdU-induced DNA damage in HL60 cells. HL60 cells were incubated with 41.3 MBq of ^{123}I -ITdU or 12.4 MBq of ^{123}I -ITdU per milliliter or were left untreated (control). After time points as indicated, alkaline electrophoresis (comet assay) was performed. (A) DNA damage measured by comet assay. (B) DNA damage quantified by fluorescence intensity of tail and nucleus, olive tail moment, at time points as indicated.

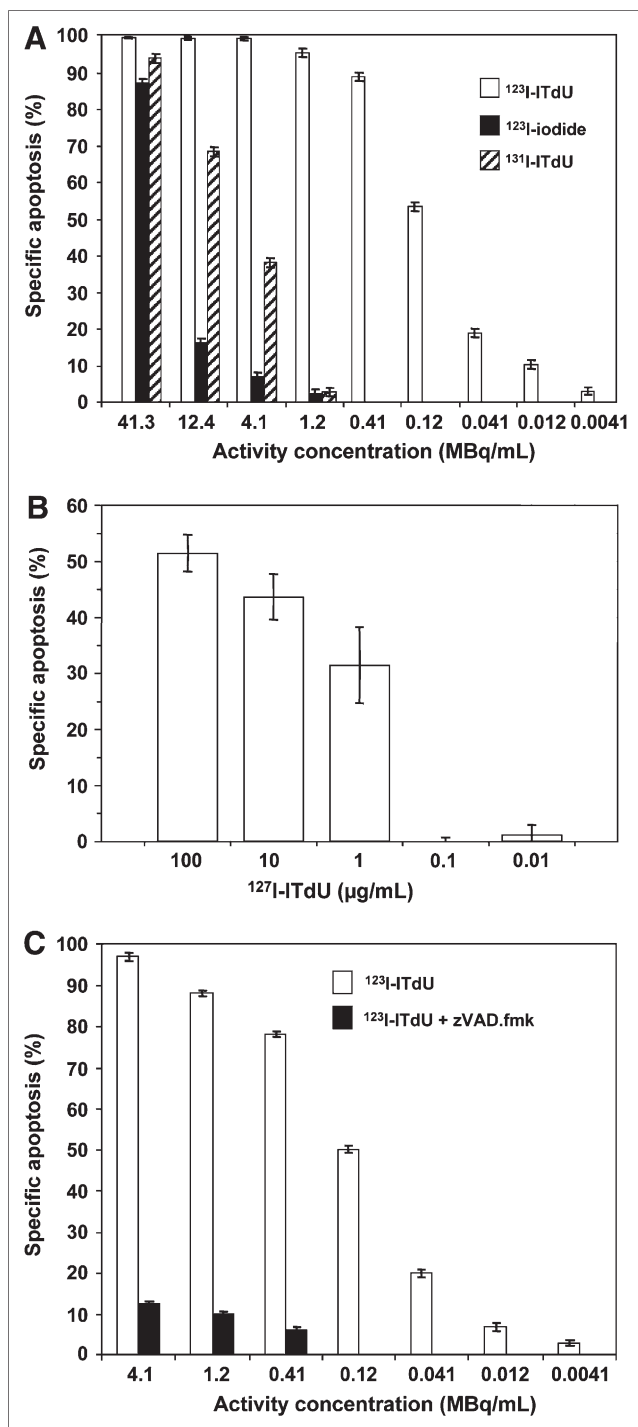


FIGURE 4. Apoptosis induction of $^{123}\text{I-ITdU}$ (Auger electron emitter bound to DNA) in HL60 cells, $^{123}\text{I-iodide}$ (Auger electron emitter not bound to DNA), and $^{131}\text{I-ITdU}$ (β -particle emitter bound to DNA). Percentages of specific cell death were analyzed after 72 h. (A) HL60 cells were incubated with indicated concentrations of $^{123}\text{I-ITdU}$, ^{123}I , or $^{131}\text{I-ITdU}$. (B) $^{127}\text{I-ITdU}$ -induced apoptosis in HL60 cells. HL60 cells were incubated with nonradioactive $^{127}\text{I-ITdU}$ at concentrations as indicated. (C) Inhibition of $^{123}\text{I-ITdU}$ -induced apoptosis by z-VAD.fmk in HL60 cells. HL60 cells were incubated with indicated concentrations of $^{123}\text{I-ITdU}$ in absence or presence of 50 μM z-VAD.fmk.

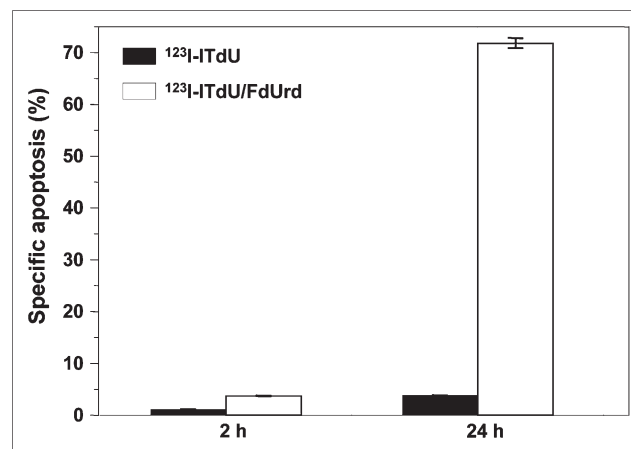


FIGURE 5. Apoptosis induction of $^{123}\text{I-ITdU}$ with and without FdUrd. HL60 cells were incubated with 0.5 MBq of $^{123}\text{I-ITdU}$ per milliliter in absence or presence of 0.01 nmol of FdUrd per liter. After 2 h and 24 h, percentages of specific cell death were analyzed.

finally to efficient tumor cell kill. Apoptosis induction was markedly amplified by inhibition of TS, thus increasing substrate flux through the thymidine salvage pathway and inhibiting TS-mediated dehalogenation of $^{123}\text{I-ITdU}$. Importantly, extremely high radiotoxicity for $^{123}\text{I-ITdU}$ was also observed in leukemia cells resistant to β - or γ -irradiation and doxorubicin.

In the present study, $^{123}\text{I-ITdU}$ was used as the molecular carrier of the Auger electron-emitting radionuclide ^{123}I . $^{123}\text{I-ITdU}$ is metabolically incorporated into DNA via the thymidine salvage pathway (7,8). This targeting approach seems promising because ENT1-type nucleoside transporters and key enzymes of the thymidine salvage pathway, major determinants of cellular $^{123}\text{I-ITdU}$ metabolism, are overexpressed in leukemic cells and many malignant tumors (23–27).

Metabolic stability is a critical requirement for incorporation of C-5 halogenated thymidine analogs into DNA. We thus followed the strategy to substitute the 4'-oxygen for sulfur in the IdUrd molecule to generate the thymidine analogs $^{123}\text{I-ITdU}$ and $^{131}\text{I-ITdU}$, with a stabilized glycosidic bond (7,8). In addition, TS-mediated dehalogenation of 5-iodo-2'-deoxyuridinemonophosphate as well as other 5-iodo- or 5-bromo-substituted deoxyuridine monophosphates is of major concern (28,29). TS catalyzed the facile dehalogenation of 5-iodo- and 5-bromo-2'-deoxyuridinemonophosphate to give the natural substrate of TS, 2'-deoxyuridinemonophosphate (29). Accordingly, we found a rapid and extensive dehalogenation of $^{123}\text{I-ITdU}$ mediated by HL60. As described for IdUrd (30), the TS inhibitor FdUrd could completely block TS-mediated dehalogenation of $^{123}\text{I-ITdU}$ in a nontoxic concentration and increase substrate flux through the thymidine salvage pathway as indicated by the 18-fold increased DNA uptake of $^{123}\text{I-ITdU}$, resulting in roughly 20-fold apoptosis induction. Because TS is overexpressed in many leukemic

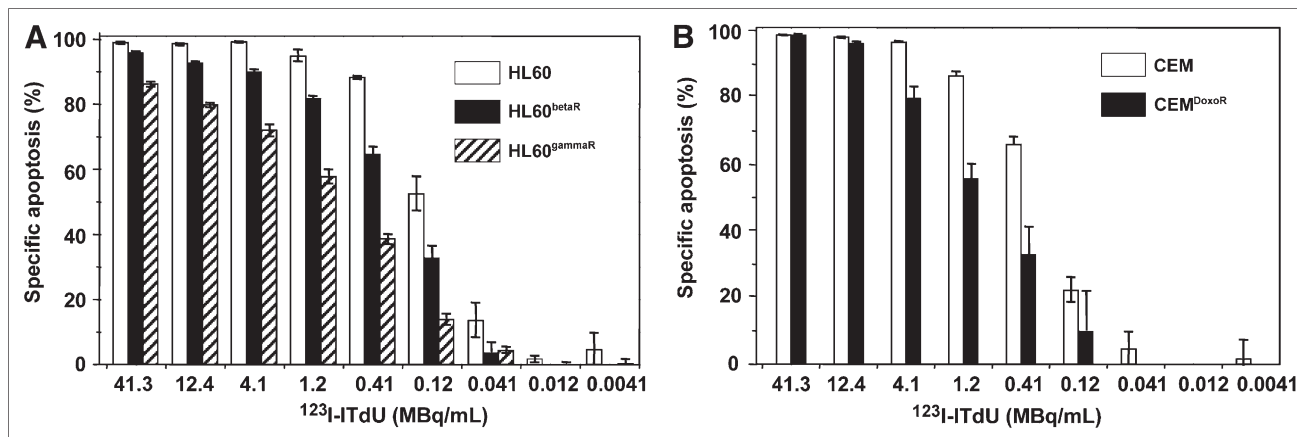


FIGURE 6. $^{123}\text{I-ITdU}$ -induced apoptosis in HL60 or CEM leukemia cells resistant to β -irradiation, γ -irradiation, or doxorubicin. Percentages of apoptotic cell death were analyzed after 72 h. (A) $^{123}\text{I-ITdU}$ -induced apoptosis in HL60^{betaR}, HL60^{gammaR}, and sensitive parental HL60 leukemia cells. HL60, HL60^{betaR}, and HL60^{gammaR} were incubated with indicated concentrations of $^{123}\text{I-ITdU}$. (B) $^{123}\text{I-ITdU}$ -induced apoptosis in CEM^{DoxoR} and parental sensitive CEM leukemia cells. CEM and CEM^{DoxoR} were incubated with indicated concentrations of $^{123}\text{I-ITdU}$.

cells and malignant tumors (31–33), a potential therapeutic use of $^{123}\text{I-ITdU}$ would almost certainly require a combination of $^{123}\text{I-ITdU}$ with FdUrd or a similar TS inhibitor.

An increased radiotoxicity of cells retained in S-phase after FdUrd pretreatment was observed by Perillo-Adamer et al. (34) in glioblastoma cell lines. However, Kassis et al. (35) found that FdUrd pretreatment does not seem to enhance the therapeutic potential of $^{125}\text{I-ITdU}$. The observation that the radiotoxicity increase was most pronounced after prolonged incubation with $^{123}\text{I-ITdU}$, thus probably targeting more cells during S-phase, might suggest that the state of cells in the cell cycle is probably relevant for the full evolution of the cytotoxic effect of Auger electron-emitting radionucleosides.

Considerably strong apoptosis and caspase-3, -8, and -9 and poly(adenosine diphosphate ribose) polymerase cleavage was observed after treatment with the DNA-bound Auger electron emitter $^{123}\text{I-ITdU}$, in contrast to the DNA-bound β -particle emitter $^{131}\text{I-ITdU}$, the nonradioactive DNA-bound $^{127}\text{I-ITdU}$, and the Auger electron emitter $^{123}\text{I-iodide}$ not bound to DNA, demonstrating the high radiotoxicity of the DNA-bound Auger electron emitter $^{123}\text{I-ITdU}$. Triggering of apoptotic cell death by a pharmacodynamic effect of $^{123}\text{I-ITdU}$ can be excluded, because the amount of $^{123}\text{I-ITdU}$ given to the incubation medium was 4–5 orders of magnitude below the cell culture infective dose (>100 $\mu\text{mol/L}$) required to reduce Vero cells by 50% over a 4-d period (13). Therefore, the cytotoxic effect of $^{123}\text{I-ITdU}$ could be attributed to Auger electron emitters bound to DNA and not to the γ -radiation component of ^{123}I or the pharmacodynamic effect of the tracer amounts of $^{127}\text{I-ITdU}$. In addition, the 150-times-higher toxicity of $^{123}\text{I-ITdU}$, compared with $^{123}\text{I-iodide}$, distributed in the extracellular space clearly emphasizes the selectivity of the Auger electron-based DNA targeting approach. In line with this observation, a higher relative biologic efficacy of ^{125}I

incorporated in DNA through radiolabeled thymidine analogs was observed, as compared with ^{125}I distributed in the cytoplasm (6).

Resistance to radiotherapy or chemotherapy is a common cause of treatment failure in cancer patients and has been linked to upregulated DNA repair pathways (36). It has been shown, however, that bulky DNA lesions, induced by Auger electrons, are only rarely or not at all repaired and preferentially trigger apoptotic cell death (5). Efficient induction of apoptotic signaling and cell death provide evidence that Auger electron emitters bound to DNA generated extensive, only rarely repairable DNA damage even in cells resistant to conventional β - or γ -irradiation or doxorubicin, used as a model for resistance to cytotoxic chemotherapy.

We have previously shown cross-resistance of γ -irradiation-resistant CEM^{gammaR} cells to doxorubicin, cisplatin, cyclophosphamide, and etoposide (37). Efficient apoptosis induction by nanoirradiation of DNA in multidrug-resistant CEM^{DoxoR} and in HL60^{betaR} or HL60^{gammaR}, resistant to β -radiation or γ -radiation, indicates the potential of nanoirradiation to overcome resistance to diverse resistance mechanisms, provided that functional integrity of executioner caspases is maintained.

CONCLUSION

These findings provide evidence that ultrasensitive nanoirradiation of DNA through Auger electron-carrying metabolic substrates offers an extremely effective strategy for inducing cell death and breaking resistance to more conventional types of irradiation or chemotherapy.

ACKNOWLEDGMENTS

This work was supported by grant KFO120 from Deutsche Forschungsgemeinschaft (German Research Foundation)

and grant DJCLS H04/05 from Deutsche Jose Carreras-Leukämie Stiftung. This work is dedicated to Professor L. E. Feinendegen.

REFERENCES

- O'Donoghue JA, Wheldon TE. Targeted radiotherapy using Auger electron emitters. *Phys Med Biol*. 1996;41:1973–1992.
- Bloomer WD, Adelstein SJ. 5-¹²⁵I-iododeoxyuridine as prototype for radionuclide therapy with Auger emitters. *Nature*. 1977;265:620–621.
- Kassis AI. Cancer therapy with Auger electrons: are we almost there? *J Nucl Med*. 2003;44:1479–1481.
- Stapanek J, Larsson B, Weinreich R. Auger-electron spectra of radionuclides for therapy and diagnostics. *Acta Oncol*. 1996;35:863–868.
- Kassis AI, Adelstein SJ. Radiobiologic principles in radionuclide therapy. *J Nucl Med*. 2005;46(suppl):S4–S12.
- Sastry KS. Biological effects of the Auger emitter iodine-125: a review—report no. 1 of AAPM Nuclear Medicine Task Group No. 6. *Med Phys*. 1992;19:1361–1370.
- Parker WB, Shaddix SC, Rose LM, et al. Metabolism and metabolic actions of 4'-thiothymidine in L1210 cells. *Biochem Pharmacol*. 1995;50:687–695.
- Toyohara J, Hayashi A, Sato M, et al. Rationale of 5-¹²⁵I-iodo-4'-thio-2'-deoxyuridine as a potential iodinated proliferation marker. *J Nucl Med*. 2002;43:1218–1226.
- Toyohara J, Gogami A, Yonekura Y, Fujibayashi Y. Pharmacokinetics and metabolism of 5-¹²⁵I-iodo-4'-thio-2'-deoxyuridine in rodents. *J Nucl Med*. 2003;44:1671–1676.
- Prusoff WH, Jaffe JJ, Gunther H. Studies in the mouse of the pharmacology of 5-iododeoxyuridine, an analogue of thymidine. *Biochem Pharmacol*. 1960;3:110–121.
- Dupertuis Y, Vazquez M, March J, et al. Fluorodeoxyuridine improves imaging of human glioblastoma xenografts with radiolabeled iododeoxyuridine. *Cancer Res*. 2001;61:7971–7977.
- Buchegger F, Perillo-Adamer F, Dupertuis YM, Bischof Delaloye A. Auger radiation targeted into DNA: a therapy perspective. *Eur J Nucl Med Mol Imaging*. 2006;33:1352–1363.
- Rahim SG, Trivedi N, Bogunovic-Batchelor MV, et al. Synthesis and anti-herpes virus activity of 2'-deoxy-4'-thiopyrimidine nucleosides. *J Med Chem*. 1996;39:789–795.
- Wirsching J, Voss J, Adiwidjaja G, Giesler A, Kopf J. Synthesis and structural elucidation of 2'-deoxy-4'-thio-L-threo-pentofuranosylpyrimidine and -purine nucleosides. *Eur J Org Chem*. 2001:1077–1087.
- Dyson MR, Coe PL, Walker RT. An improved synthesis of benzyl 3,5-di-O-benzyl-2-deoxy-1,4-dithio-D-erythro-pentofuranoside, an intermediate in the synthesis of 4'-thionucleosides. *Carbohydr Res*. 1991;216:237–248.
- Friesen C, Glatting G, Koop B, et al. Breaking chemo- and radioresistance with [²¹³Bi]anti-CD45 antibodies in leukemia cells. *Cancer Res*. 2007;67:1950–1958.
- Friesen C, Kiess Y, Debatin KM. A critical role of glutathione in determining apoptosis sensitivity and resistance in leukemia cells. *Cell Death Differ*. 2004;11(suppl 1):S73–S85.
- Hartmann A, Agurell E, Beevers C, et al. Recommendations for conducting the in vivo alkaline Comet assay: 4th International Comet assay workshop. *Mutagenesis*. 2003;18:45–51.
- Nicoletti I, Migliorati G, Pagliacci MC, Grignani F, Riccardi C. A rapid and simple method for measuring thymocyte apoptosis by propidium iodide staining and flow cytometry. *J Immunol Methods*. 1991;139:271–279.
- Friesen C, Lubatschowski A, Kotzerke J, Buchmann I, Reske SN, Debatin K-M. Beta-irradiation used for systemic radioimmunotherapy induces apoptosis and activates apoptosis pathways in leukemia cells. *Eur J Nucl Med Mol Imaging*. 2003;30:1251–1261.
- Unak P, Cetinkaya B. Absorbed dose estimates at the cellular level for ¹³¹I. *Appl Radiat Isot*. 2005;62:861–869.
- Friesen C, Fulda S, Debatin K-M. Deficient activation of the CD95 (APO-1/Fas) system in drug-resistant cells. *Leukemia*. 1997;11:1833–1841.
- Belt JA, Marina NM, Phelps DA, Crawford CR. Nucleoside transport in normal and neoplastic cells. *Adv Enzyme Regul*. 1993;33:235–252.
- Mackey JR, Baldwin SA, Young JD, Cass CE. Nucleoside transport and its significance for anticancer drug resistance. *Drug Resist Update*. 1998;1:310–324.
- Ellims PH, Gan TE, Van-der-Weyden MB. Thymidine kinase isoenzymes in chronic lymphocytic leukaemia. *Br J Haematol*. 1981;49:479–481.
- Eriksson S, Munch-Petersen B, Johansson K, Eklund H. Structure and function of cellular deoxyribonucleoside kinases. *Cell Mol Life Sci*. 2002;59:1327–1346.
- Ackland SP, Peters GJ. Thymidine phosphorylase: its role in sensitivity and resistance to anticancer drugs. *Drug Resist Update*. 1999;2:205–214.
- Wataya Y, Santi DV, Hansch C. Inhibition of Lactobacillus casei thymidylate synthetase by 5-substituted 2'-deoxyuridylates: preliminary quantitative structure-activity relationship. *J Med Chem*. 1977;20:1469–1473.
- Garrett C, Wataya Y, Santi DV. Thymidylate synthetase: catalysis of dehalogenation of 5-bromo- and 5-iodo-2'-deoxyuridylate. *Biochemistry*. 1979;18:2798–2804.
- Buchegger F, Adamer F, Schaffland AO, et al. Highly efficient DNA incorporation of intratumorally injected [¹²⁵I]iododeoxyuridine under thymidine synthesis blocking in human glioblastoma xenografts. *Int J Cancer*. 2004;110:145–149.
- van Triest B, Pinedo HM, Blauwgeers JL, et al. Prognostic role of thymidylate synthase, thymidine phosphorylase/platelet-derived endothelial cell growth factor, and proliferation markers in colorectal cancer. *Clin Cancer Res*. 2000;6:1063–1072.
- Rooseboom M, Commandeur JN, Vermeulen NP. Enzyme-catalyzed activation of anticancer prodrugs. *Pharmacol Rev*. 2004;56:53–102.
- Romain S, Bendahl PO, Guirou O, Malmstrom P, Martin PM, Ferno M. DNA-synthesizing enzymes in breast cancer (thymidine kinase, thymidylate synthase and thymidylate kinase): association with flow cytometric S-phase fraction and relative prognostic importance in node-negative premenopausal patients. *Int J Cancer*. 2001;95:56–61.
- Perillo-Adamer F, Bischof Delaloye A, Genton CS, Schaffland AO, Dupertuis YM, Buchegger F. Short fluorodeoxyuridine exposure of different human glioblastoma lines induces high-level accumulation of S-phase cells that avidly incorporate ¹²⁵I-iododeoxyuridine. *Eur J Nucl Med Mol Imaging*. 2006;33:613–620.
- Kassis AI, Guptill WE, Taube RA, Adelstein SJ. Radiotoxicity of 5-[¹²⁵I]iodo-2'-deoxyuridine in mammalian cells following treatment with 5-fluoro-2'-deoxyuridine. *J Nucl Biol Med*. 1991;35:167–173.
- Christmann M, Tomicic MT, Roos WP, Kaina B. Mechanisms of human DNA repair: an update. *Toxicology*. 2003;193:3–34.
- Los M, Herr I, Friesen C, Fulda S, Schulze-Osthoff K, Debatin K-M. Cross-resistance of CD95- and drug-induced apoptosis as a consequence of deficient activation of caspases (ICE/Ced-3 proteases). *Blood*. 1997;90:3118–3129.



The Journal of
NUCLEAR MEDICINE

^{123}I -ITdU-Mediated Nanoirradiation of DNA Efficiently Induces Cell Kill in HL60 Leukemia Cells and in Doxorubicin-, β -, or γ -Radiation-Resistant Cell Lines

Sven N. Reske, Sandra Deisenhofer, Gerhard Glatting, Boris D. Zlatopolskiy, Agnieszka Morgenroth, Andreas T. J. Vogt, Andreas K. Buck and Claudia Friesen

J Nucl Med. 2007;48:1000-1007.
Published online: May 15, 2007.
Doi: 10.2967/jnumed.107.040337

This article and updated information are available at:
<http://jnm.snmjournals.org/content/48/6/1000>

Information about reproducing figures, tables, or other portions of this article can be found online at:
<http://jnm.snmjournals.org/site/misc/permission.xhtml>

Information about subscriptions to JNM can be found at:
<http://jnm.snmjournals.org/site/subscriptions/online.xhtml>

The Journal of Nuclear Medicine is published monthly.
SNMMI | Society of Nuclear Medicine and Molecular Imaging
1850 Samuel Morse Drive, Reston, VA 20190.
(Print ISSN: 0161-5505, Online ISSN: 2159-662X)

© Copyright 2007 SNMMI; all rights reserved.

The logo for the Society of Nuclear Medicine and Molecular Imaging (SNMMI) consists of the letters 'S', 'N', 'M', and 'I' arranged in a 2x2 grid. Each letter is white and set within a red square. To the right of this grid, the full name of the society is written in a sans-serif font: 'SOCIETY OF NUCLEAR MEDICINE AND MOLECULAR IMAGING'.

SOCIETY OF
NUCLEAR MEDICINE
AND MOLECULAR IMAGING